THE EFFECT OF USING ALUMINIUM FOAM IN STEEL SANDWICH TARGETS AGAINST BLUNT PROJECTILES

Mohamed Hassan Abdelshafy

Faculty member in Mech. Dept., Military Technical College, Cairo, Egypt

m.abdelshafy@mtc.edu.eg

Abstract

In this paper, the effect of using Aluminium Foam (Alporas) on the ballistic resistance of multi layered target comprising two steel layers and Al foam in between against rigid projectile of blunt nose impact at sub-ordnance velocities (320 : 400 m/s) is evaluated using finite element analysis using ABAQUS/explicit. Rigid projectile of blunt nose is considered, it is manufactured from Arne tool steel with a nominal mass and diameter of 197 g and 20 mm. The evaluation has been done by comparing the ballistic resistance of a single layer of steel plate to eleven different composite plate structure comprising two layers of steel plates and Aluminium foam layer sandwiched between them. The study reveals that using Aluminium foam absorbs more kinetic energy from the projectile during penetration and, hence, reduces the residual velocity of the projectile. Also it is found that the total mass of each structure is less than the total mass of single layer target.

Key Words

Impact, Aluminium Foam, Abaqus, Armox

1. Introduction

Armour design is an important feature into development of more protective systems against the threat of projectiles. Traditionally, armour has been made of monolithic steel of high strength, although the rolled armor steel is remaining the most widely used material. The need for obtaining lightweight armor has led to the investigation of new materials. Such materials are needed to improve the ballistic resistance as well as reduce the weight of existing armor. Recently cellular core materials like aluminium foam have been investigated to achieve more energy absorbent structure.

For example, aluminium foam is used in the front of aircrafts to prevent accidental bird strikes [1], which can cause major damage to planes and therefore affect their safety. An important objective of this protection is to avoid the perforation of panels, which can cause the depressurization of aircrafts. Penetration/perforation resistances at high impact velocity of sandwich panels are then required to qualify different panels made of different skin materials (aluminium, fire-reinforced polymer) and cellular cores (honeycomb, foam, hollow sphere, etc.).

Common penetration tests for lower velocity (< 15 m/s) could be performed using a drop hammer with a perforator [2, 3]. The basic measurement in this case is the deceleration of the impact mass, estimated by an accelerometer. The force–displacement curves can be derived even though they are sometimes not accurate enough. However, the common testing technique at higher velocity consists in launching with a gas gun a free flying projectile against target [4-6]. Such a way is also used in the case of sandwich targets [7, 8].

The main measures were velocities before and after perforation of the panel and there was a lack of whole perforating force-displacement history. One can only have a global energy absorbed during penetration [8, 9] and this makes understanding of what was happened during high-speed perforation processes very difficult.

The aim of this paper is to evaluate the effectiveness of using Aluminium foam in steel structure target on the ballistic resistance of the whole target compare to single steel layer targets at different impact velocity ranged 320:400 m/s achieved by rigid blunt projectile, the study has been done using FEA using ABAQUS/explicit [10].

2. Problem Formulation

The aim of this paper is to assess the ballistic resistance of an armour plate consisting of two steel layers and aluminium foam layer sandwiched between them. The performance of such a system will be compared to that of a monolithic plate. For that reason, several impact scenarios are considered by changing the impact velocity and the thickness of steel layers. Figure 1 shows one of the eleven scenarios of different combinations of steel and Al-foam target and in Table 1. the whole composite plate configurations are shown. Also, the impact velocity of the projectiles varies from Vi = 320 to 400m/s. The perforation resistance of the nine composite plates is evaluated by comparing their residual velocities.

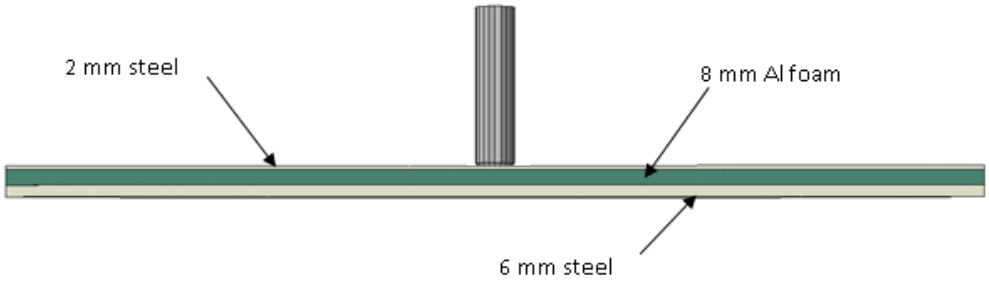

Figure 1 proposed configuration of scenario with 2mm steel+8mm Al-foam+6mm steel

Table 1 Proposed Configuration for the eleven scenarios

	Thickness of Face Plate (mm)	Thickness of Al-Foam plate (mm)	Thickness of back plate (mm)
	2	8 mm (for all configuration)	6
	3		5
	3		6
	4		4
	4		5
	4		6
	5		5
	5		6
	6		3
	6		4
	6		5

3. Plasticity Model

3.1 Steel Layer

The computational model of visco-plasticity used to predict steel behavior under projectile impact loading has earlier been presented by Borvik et al. [11]. Thus, only the main equations will be given in the following. The model is based on work by J. & C. [12] and Camacho and Ortiz [13].

J. & C. hardening is a particular type of isotropic hardening where the yield stress at nonzero strain rate, $\bar{\sigma}$, is assumed to be of the form

$$\bar{\sigma} = \left[A + B(\bar{\varepsilon}^{pl})^n\right]\left[1 + C\ \ln\left(\frac{\dot{\bar{\varepsilon}}^{pl}}{\dot{\varepsilon}_0}\right)\right](1-\hat{\theta}^m) \qquad (1)$$

Where A, B, n and m are material parameters measured at or below the transition temperature $\theta_{transition}$,. $\hat{\theta}$ is the nondimensional temperature defined as

$$\hat{\theta} \equiv \begin{cases} 0 & for\ \theta \prec \theta_{transition} \\ (\theta - \theta_{transition})/(\theta_{melt} - \theta_{transition}) & for\ \theta_{transition} \le \theta \le \theta_{melt} \\ 1 & for\ \theta \succ \theta_{melt} \end{cases} \qquad (2)$$

where θ is the current temperature, θ_{melt} is the melting temperature, and $\theta_{transition}$ is the transition temperature defined as the one at or below which there is no temperature dependence on the expression of the yield stress.

Where $\dot{\bar{\varepsilon}}^{pl}$ is the equivalent plastic strain rate

$$\dot{\bar{\varepsilon}}^{pl} = \dot{\varepsilon}_0 \exp\left[\frac{1}{C}(R-1)\right] \quad for\ \bar{\sigma} \ge \sigma^0 \qquad (3)$$

Where $\dot{\varepsilon}_0$ and C are material parameters measured at or below the transition temperature, $\theta_{transition}$, and where σ^0 is the static yield stress

$$\sigma^0 = \left[A + B(\bar{\varepsilon}^{pl})^n\right](1-\hat{\theta}^m) \qquad (4)$$

Weldox steel is of high strength and of outstanding ductility. To study the mechanical properties of Weldox 460 E steel, a series of static and dynamic tensile measurements were done by Borvik et al. [14, 15]. Table 3 gives the values of all of the material constants

In the fracture model, a damage initiation criterion for fracture of metals has been used which used in combination with the damage evolution models for ductile metals. The model assumes that the equivalent plastic strain at the onset of damage, $\bar{\varepsilon}_D^{pl}$, is a function of stress triaxiality and strain rate $\bar{\varepsilon}_D^{pl}\left(\eta, \dot{\bar{\varepsilon}}^{pl}\right)$, where $\eta = -p/q$, is the stress triaxiality, p is the pressure stress, q is the Mises equivalent stress, and $\dot{\bar{\varepsilon}}^{pl}$ is the equivalent plastic strain rate. The criterion for damage initiation is met when the following condition is satisfied:

$$\omega_D = \int \frac{d\bar{\varepsilon}^{pl}}{\bar{\varepsilon}_D^{pl}\left(\eta, \dot{\bar{\varepsilon}}^{pl}\right)} = 1 \qquad (5)$$

where ω_D is a state variable that increases monotonically with plastic deformation. At each increment during the analysis the incremental increase in is computed as:

$$\Delta\omega_D = \frac{\Delta\bar{\varepsilon}^{pl}}{\bar{\varepsilon}_D^{pl}\left(\eta, \dot{\bar{\varepsilon}}^{pl}\right)} \geq 1 \qquad (6)$$

3.2 Aluminium Foam Layer

The Mises yield surface is used to define isotropic yielding. It is defined by giving the value of the uniaxial yield stress as a function of uniaxial equivalent plastic strain. Although there is crushable foam model implemented in ABAQUS/explicit but it still not completely well defined specially at high strain rate problem; so that an isotropic hardening is defined in which the yield stress is given as a tabular function of plastic strain Figure 2, Table 4 gives the values of all of the material constants.

Also, it is assumed that the Al-Foam will fail as aluminium failure, which will be defined as damage initiation criteria for fracture of metals combined with damage evolution models for ductile metals. The triaxiality ratio versus fraction strain curve of aluminium measured by [16] is used to define the Al-foam failure as shown in Table 2.

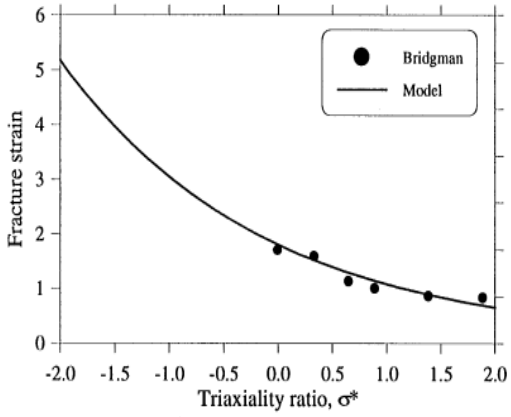

Figure 2 Calibration of material model

Table 2 Measured values of fracture strain as a function of stress triaxiality ratio [16]

Fracture strain	Triaxiality ratio
0.929	0.333
0.497	0.893
0.364	1.389
0.197	1.891

Table 3 Preliminary model constants for Weldox 460 E steel [11]

Elastic constants and density		
E (GPa)	ν	ρ (Kg/m^3)
200	0.33	7850
Yield stress and strain hardening		
A (MPa)	B (MPa)	n
490	807	0.73
Strain rate hardening		**Damage evolution**

$\dot{\varepsilon}_o$ (s^{-1})	C	D_c	p_d
5.10^{-4}	0.012	0.30	0

Table 4 Model constant for Al-Foam (Alporas)

E (GPa)	ν	ρ (Kg/m^3)
1.1	0.33	250

4. Computational Model

Most of the previous numerical studies of structural impact have been performed using the code LS-DYNA. In the present study the ABAQUS [10] has been used. The code includes a general purpose finite element program (ABAQUS/standard), and an explicit finite element program (ABAQUS/explicit). The latter uses a central difference time integration rule to efficiently analyze incremental deformation. An explicit central difference operator satisfies the dynamic equilibrium equations at the beginning of the increment, t. The accelerations calculated at time t are used to advance the velocity solution to time t+Δt/2 and the displacement solution to time t+Δt.

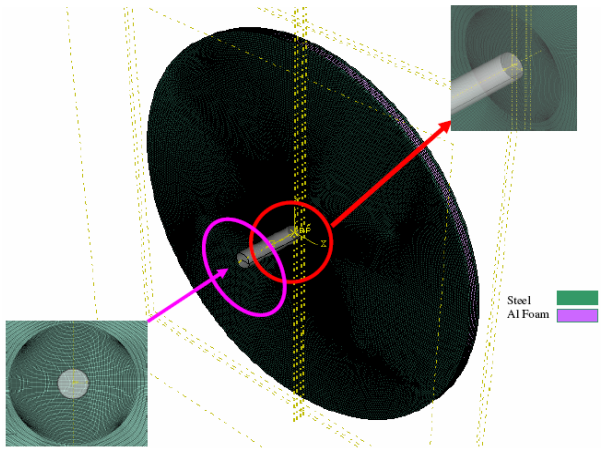

Figure 3 Finite element model of composite structure target (steel + Al-Foam + steel)

To achieve the objective, a 3D model was created by using the pre-processing module of the ABAQUS code. The target plates, both Steel and Al-Foam, were modelled as deformable bodies and material properties were assigned to it as discussed earlier. The projectile was modelled as a rigid part. A single node reference point was used to assign mass and initial velocity. Eight-node brick elements with reduced integration, which are denoted by C3D8R, were used in the analysis.

The mesh was refined in the penetration zone. The mesh density was reduced as the distance from the impact area increased. In this simulations, the radius of the circular plate is 250mm, the thickness of monolithic target is 12 mm, and as shown in Figure 3 the total thickness of the composite structure varies. Each structure consists of two steel layers and 8mm thick of Al-Foam sandwiched between them, the face layer thickness varies from 3mm to 6mm, and the back layer thickness varies from 4mm to 6mm. Clamped boundary condition are assumed at the periphery of the plate.

General contact between the projectile and the plates

was modelled by using a kinematic contact algorithm. The effect of friction between projectile and target is considered between the projectile and the target plates and is assumed to be 0.1.

5. Computational Results

Simulations of impact of single steel layer target and nine composite structures targets consist of steel and Al-foam by blunt projectile were carried out at impact velocities 320 to 400 m/s. Figure 4 shows the effect of using different target configuration on the projectile velocity profile during the penetration process through the whole target.

Figure 4-a shows the predicted projectile velocity profiles during the penetration process into the sandwich panel targets at impact velocity of 400 m/s. The sandwich panel are of different configurations of total thickness of 16 mm, the configurations of the targets are (2+8+6), (3+8+5) and (4+8+4), where the first number denotes the thickness of the face plate, the second number denotes the thickness of the Al-foam layer and the third number denotes the thickness of the back plate. They are compared with the projectile velocity profiles for the single layer targets to illustrate the effect of using sandwich panel targets on the projectile velocity profile and, hence, the projectile residual velocity. From the figure, the sandwich panel target with configuration (4+8+4) is the best because it has the lowest residual velocity and, therefore, the projectile perforates the targets with the lowest velocity than the other target configurations

Figure 4-b shows the predicted projectile velocity profiles during the penetration process into the sandwich panel targets at impact velocity of 400 m/s. The sandwich panel targets are of different configurations of total thickness of 17 mm, the configurations of the targets are (3+8+6), (4+8+5) and (6+8+3). They are compared with the projectile velocity profiles for the single layer targets to illustrate the effect of using sandwich panel targets on the projectile velocity profile and, hence, the projectile residual velocity. From the figure, the sandwich panel target with configuration 4+8+5 is the best because it has the lowest residual velocity and, therefore, the projectile perforates the targets with the lowest velocity than the other target configurations

Figure 4-c shows the predicted projectile velocity profiles during the penetration process into the sandwich panel targets at impact velocity of 400 m/s. The sandwich panel targets are of different configurations of total thickness of 18 mm, the configurations of the targets are (4+8+6), (5+8+5) and (6+8+4). They are compared with the projectile velocity profiles for the single layer targets to illustrate the effect of using sandwich panel targets on the projectile velocity profile and, hence, the projectile residual velocity. From the figure, the sandwich panel target with configuration 5+8+5 is the best because it has the lowest residual velocity and, therefore, the projectile perforates the targets with the lowest velocity than the other target configurations

Figure 4-d shows the predicted projectile velocity profiles during the penetration process into the sandwich panel targets at impact velocity of 400 m/s. The sandwich panel targets are of different configurations of total thickness of 19 mm, the configurations of the targets are 5+8+6) and (6+8+5). They are compared with the projectile velocity profiles for the single layer targets to illustrate the effect of using sandwich panel targets on the projectile velocity profile and, hence, the projectile residual velocity. The figure shows that, for the impact velocity of 400 m/s the target configuration (6+8+5) is better than the configuration (5+8+6) as it has lower residual velocity.

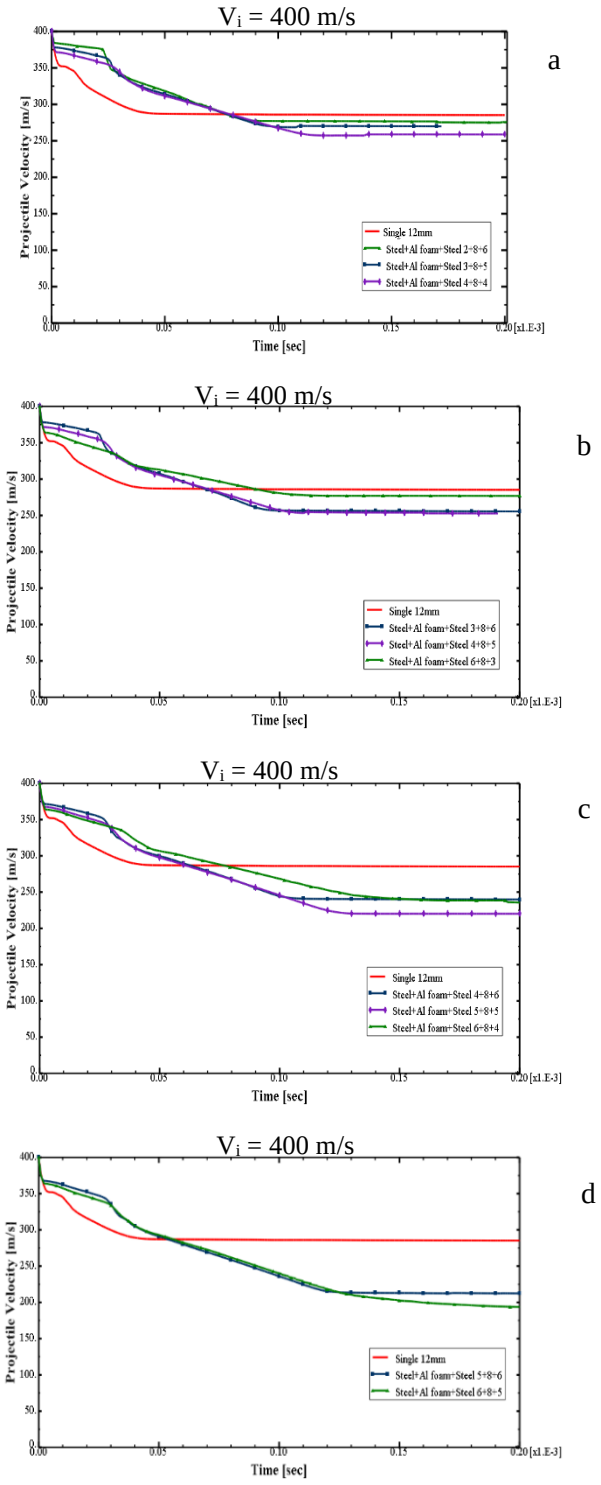

Figure 4 Effect of using different target configurations on

projectile velocity profile for impact velocity of 400 m/s

Figure 5a shows the predicted residual velocities for different impact velocities for 12 mm thick single steel targets and sandwich panel targets of total thickness of 16 mm. The sandwich panel targets are designated (2+8+6), (3+8+5) and (4+8+4) where, as stated previously the first number denotes the thickness of the front face plate of the target which is first impacted by the projectile, and the third number denotes the back face plate of the target.

It is observed that using sandwich panel targets with different configurations resulted in decrease in the residual velocity. Hence, the sandwich panel targets have better penetration resistance than the single layer target. Figure 5-a shows that the sandwich panel target of configuration (4+8+4) reduced the residual velocity compared with the 12 mm single layer steel targets by about 9.5 % at impact velocity of 400 m/s and by about 14.9 % at impact velocity of 340 m/s. Also, the weight saving, one of the important factors in target design, when the single 12 mm steel target is substituted by the (4+8+4) sandwich panel is about 31.2%.

Figure 5-b shows the predicted residual velocities for different impact velocities for 12 mm thick single steel targets and sandwich panel targets of total thickness of 17 mm. The sandwich panel targets are designated (3+8+6), (4+8+5) and (6+8+3). It is found that the sandwich panel targets have lower residual velocities than those of the single layer targets. In addition, the figure shows that the sandwich panel target of configuration (4+8+5) has the best penetration resistance as it reduced the residual velocity compared with the 12 mm single layer steel targets by about 11.6 % at impact velocity of 400 m/s and by about 31.4 % at impact velocity of 320 m/s. Furthermore, the weight saving is about 22.9 %.

Also, Figure 5-c compares the predicted residual velocities for different impact velocities for 12 mm thick single steel targets to those for the sandwich panel targets of total thickness of 18 mm. The sandwich panel targets are designated (4+8+6), (5+8+5) and (6+8+4). The figure shows that all configurations have better effect on the residual velocities than the single layer target, and at the impact velocity of 400 m/s the sandwich panel targets of configuration (5+8+5) is the best and at the impact velocity of 340 m/s the projectile is embedded inside each target. Figure 5-c shows that the sandwich panel target of configuration (5+8+5) reduced the residual velocity compared with the 12 mm single layer steel targets by about 23 % at impact velocity of 400 m/s and the weight saving is about 14.5 %.

Figure 5-d shows the comparison between the predicted residual velocities for different impact velocities for 12 mm thick single steel targets and those for the sandwich panel targets of total thickness of 19 mm. The sandwich panel targets are designated (5+8+6), and (6+8+5). The figure shows that both configurations have better effect on the residual velocities than the single layer target, and at the impact velocity of 400 m/s the sandwich panel targets of configuration (6+8+5) is the best, while for impact velocities of 380 and 360 m/s the target of configuration (5+8+6) is the best. At impact velocity of 340 m/s the projectile is embedded inside both targets. Furthermore, the weight saving, when the sandwich panel target of total thickness of 19 mm is used instead of a single layer steel target is 6.2 %.

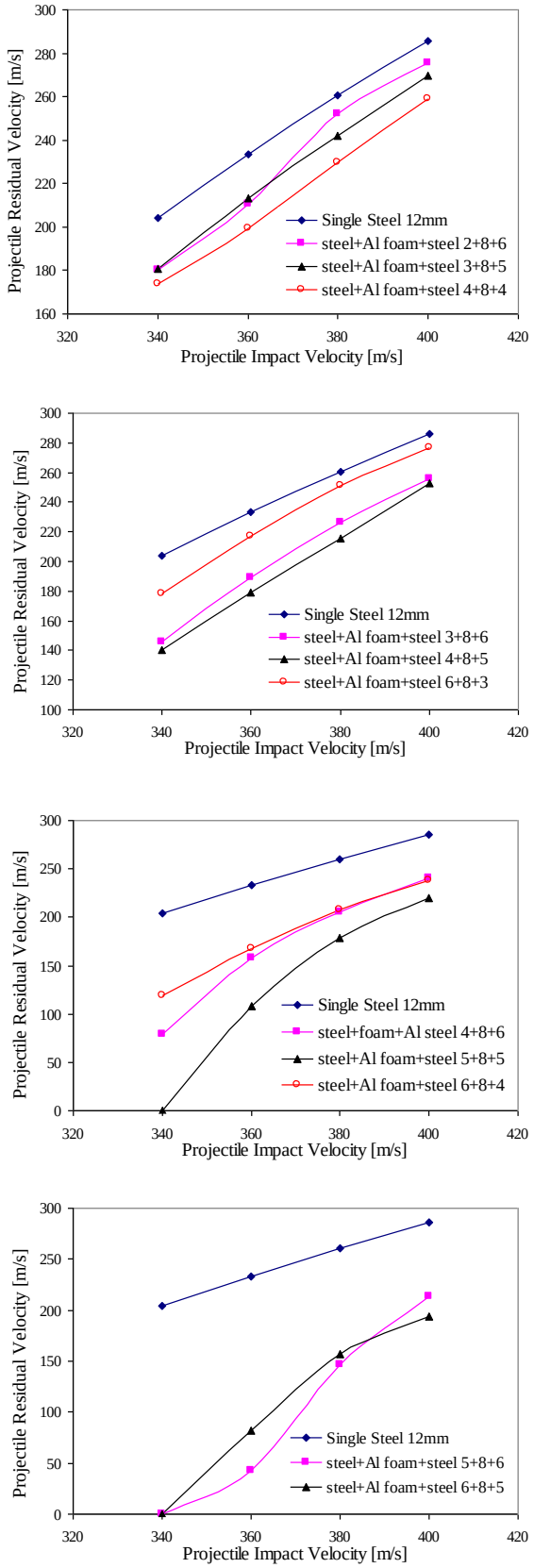

Figure 5 Comparison between the Projectile Residual velocities at Different Impact velocities of Single Steel Target of 12 mm thickness and Targets of different Configurations

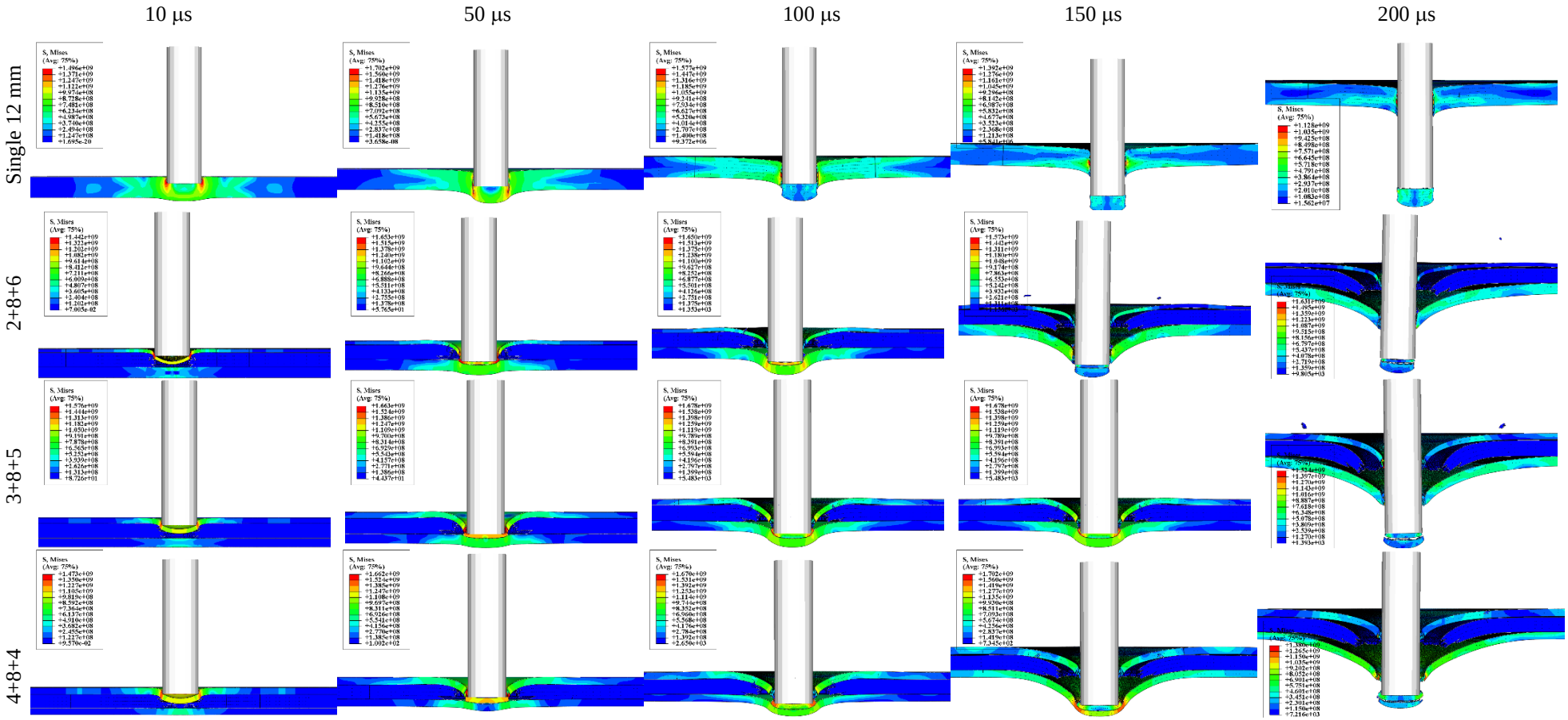

Figure 6 Predicted von Mises Stress Contours for Target Configuration of total thickness of 16mm compared with the 12 mm single steel target

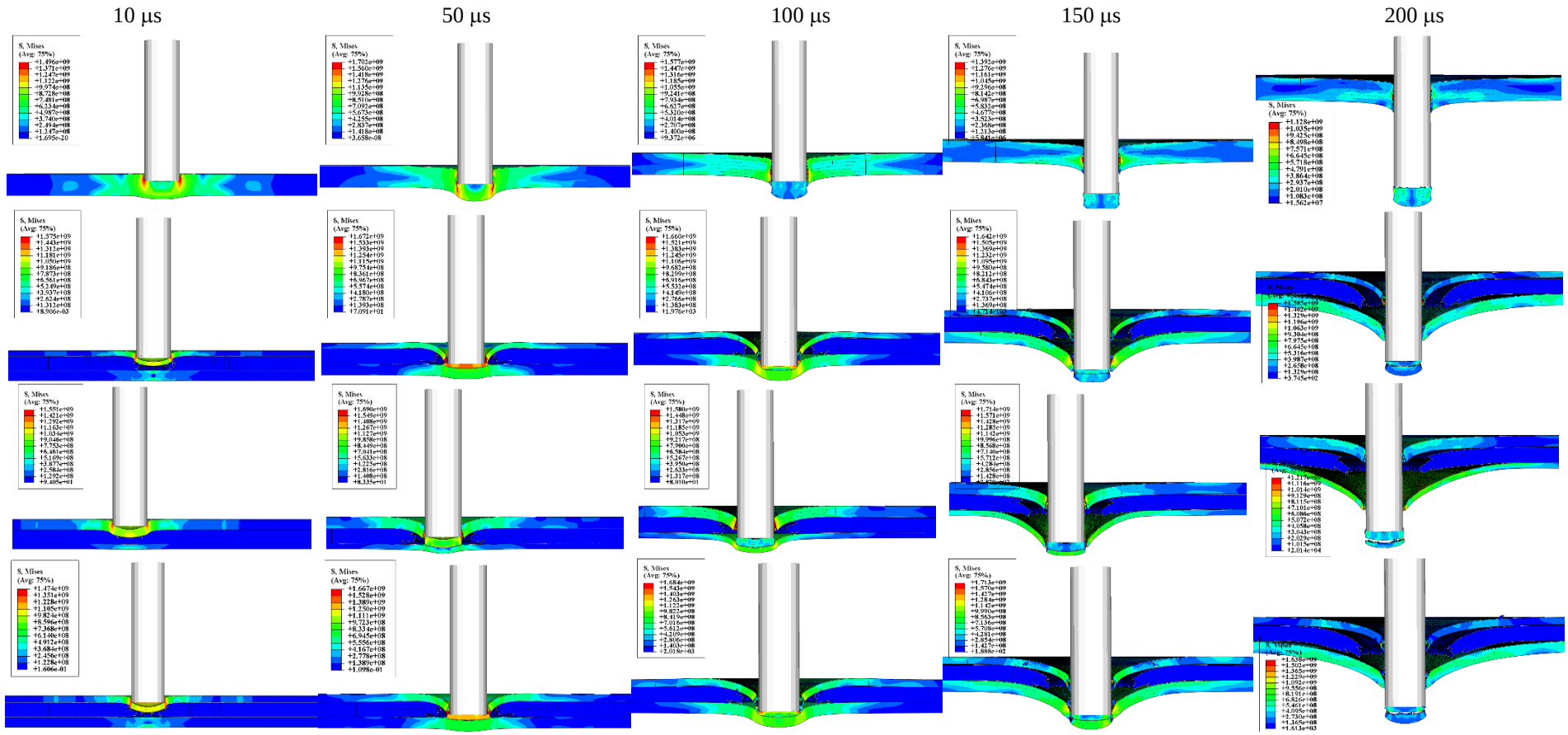

Figure 7 Predicted von Mises Stress Contours for Target Configuration of total thickness of 17mm compared with the 12 mm single steel target

Error! Reference source not found. and **Error! Reference source not found.** show the predicted von-Mises stress contours during projectile penetration into the sandwich panel targets of total thickness of 16 and 17 mm at impact velocity of 400 m/s, respectively. Also, the predicted von-Mises stress contours during projectile penetration into the 12 mm thick single steel target are shown in each figure in order to show the difference through the penetration process at different time.

Error! Reference source not found. shows the predicted von-Mises stress contours during projectile penetration into the sandwich panel targets of total thickness of 16 compared with that of 12mm thick single steel target. The figure shows that shear plugging is the predominant failure mode in the single steel target. Crack formation and propagation is often induced by the blunt corner of the flat-ended projectile. Also, the targets undergo insignificant global deformation and the plastic deformation is localized in the impacted zone. Furthermore, the figure shows that the stress contours for the Al-foam layers are always low because of the lower stiffness of the Al-foam material compared to the stiffness of the steel as it is clear from comparing the modulus of elasticity of both materials.).

It is clear that, at the initial stage of penetration (10 μsec), the first layer is greatly deformed, while the back plate is still un-deformed, although there are stresses induced in the back plate due to the wave propagation through the Al-foam. Also, it is clear that at 30 μsec time interval, the projectile and the mass segments sheared off from the first layer and from the compressed Al-foam layer began to penetrate the back plate.

Error! Reference source not found. shows the predicted von-Mises stress contours at different time intervals during the penetration process through different sandwich panel targets of different configurations of total thickness of 17 mm at impact velocity of 400 m/s. Following the same trend as the previous figure, the figure shows that the stress contours for the Al-foam layers are always low. In addition, the effect of face and back plate arrangement is shown. Furthermore, the figure shows that, when the thin plate is put in the back the penetration resistance is worse than when the thick plate is put in the back plate.

6. Conclusion

Using of Aluminium foam in multilayered structure improves the ballistic resistance of the structure compared to the single layer of the same face and back material of the structure. For different impact velocity of 20mm diameter rigid projectile with mass of 197 g, ranged from 320 :400 m/s into eleven composite structure targets comprising two steel layers and Al-Foam (Alporas) in between steel layers, it is found that the residual velocity of all nine structures is less than that for the single steel layer. Also it is found that the total mass of each structure is less than the total mass of single layer target by from 6% for 5mm steel+8mm Al-Foam+6mm steel target to 39.5% for 3mm steel+8mm Al-Foam+4mm steel target.

References

[1] Hanssen, A.G., et al., A numerical model for bird strike of aluminium foam-based sandwich panels. *International Journal of Impact Engineering*, 2006. **32**(7): p. 1127-1144.

[2] Mines, R.A.W., C.M. Worrall, and A.G. Gibson, LOW VELOCITY PERFORATION BEHAVIOUR OF POLYMER COMPOSITE SANDWICH PANELS. *International Journal of Impact Engineering*, 1998. **21**(10): p. 855-879.

[3] Shyr, T.-W. and Y.-H. Pan, Low velocity impact responses of hollow core sandwich laminate and interply hybrid laminate. *Composite Structures*, 2004. **64**(2): p. 189-198.

[4] Borvik, T., et al., Perforation of AA5083-H116 aluminium plates with conical-nose steel projectiles--experimental study. *International Journal of Impact Engineering*, 2004. **30**(4): p. 367-384.

[5] Corbett, G.G., S.R. Reid, and W. Johnson, Impact loading of plates and shells by free-flying projectiles: A review. *International Journal of Impact Engineering*, 1996. **18**(2): p. 141-230.

[6] Backman, M.E. and W. Goldsmith, The mechanics of penetration of projectiles into targets. *International Journal of Engineering Science*, 1978. **16**(1): p. 1-99.

[7] Goldsmith, W., et al., Perforation of cellular sandwich plates. *International Journal of Impact Engineering*, 1997. **19**(5-6): p. 361-379.

[8] Roach, A.M., K.E. Evans, and N. Jones, The penetration energy of sandwich panel elements under static and dynamic loading. Part I. *Composite Structures*, 1998. **42**(2): p. 119-134.

[9] Li, Y., J.B. Li, and R. Zhang, Energy-absorption performance of porous materials in sandwich composites under hypervelocity impact loading. *Composite Structures*, 2004. **64**(1): p. 71-78.

[10] Hibbitt, H., B. Karlsson , and S. P., Abaqus User's manual, ABAQUS/EXPLICIT 6.6. 2006.

[11] Borvik, T., et al., Ballistic penetration of steel plates. *International Journal of Impact Engineering*, 1999. **22**(9-10): p. 855-886.

[12] Johnson, G.R. and W.H. Cook, Fracture characteristics of three metals subjected to various strains, strain rates, temperatures and pressures. *Engineering Fracture Mechanics*, 1985. **21**(1): p. 31-48.

[13] Camacho, G.T. and M. Ortiz, Adaptive Lagrangian modelling of ballistic penetration of metallic targets. *Computer Methods in Applied Mechanics and Engineering*, 1997. **142**(3-4): p. 269-301.

[14] Borvik, T., et al., A computational model of viscoplasticity and ductile damage for impact and penetration. *European Journal of Mechanics - A/Solids*, 2001. **20**(5): p. 685-712.

[15] Borvik, T., et al., Numerical simulation of plugging failure in ballistic penetration. *International Journal of Solids and Structures*, 2001. **38**(34-35): p. 6241-6264.

[16] Gupta, N.K., M.A. Iqbal, and G.S. Sekhon, Experimental and numerical studies on the behavior of thin aluminum plates subjected to impact by blunt- and hemispherical-nosed projectiles. *International Journal of Impact Engineering*, 2006. **32**(12): p. 1921-1944.